

ANALYTICAL SOLUTION OF NON-LINEAR BOUNDARY VALUE PROBLEM FOR MHD FLOW

N.D. Vishnu Priya

Dhanalaksmi Srinivasan College of engineering, Coimbatore

V Ananthaswamy

The Madura College, Madurai, Tamil Nadu, India

M Kalaivani

The Madura College, Madurai, Tamil Nadu, India

M Subha

MSNPM Women's College, Poovanthi, Tamil Nadu, India.

Pawan Kumar Verma

Babu Banarasi Das University, Lucknow (U.P.) India

Naveen Kumar

SGT University, Gurgaon (Haryana) India

Abstract

In this paper, we investigate analytically the steady incompressible viscous MHD asymmetric flow of an electrically conducting fluid between two infinite parallel stationary coaxial porous disks of different permeability in the presence of a transverse magnetic field. The governing steady boundary layer equations are reduced to dimensionless form by similarity transformations. The approximate analytical expressions of the dimensionless axial velocity and dimensionless radial velocity are derived by using the New Homotopy analysis method. The results are presented in tabular and graphical forms to discuss important features of the flow. The Homotopy analysis method can be easily extended to solve other non-linear MHD viscous flow problems in engineering and applied sciences.

Keywords: MHD flow; Porous disks; Shear stress; Non-linear boundary value problem; New Homotopy analysis method.

Introduction

In the recent years, the investigation of flow over a stretching surface has attracted the attention of research community due to its significant applications in different industries such as extrusion paper production, extrusion of polymer sheets, metal and plastic industries [2]. Fang *et al.* [3] determined exact solution of the Navier Stokes equations analytically to study the MHD viscous flow under slip conditions over a permeable stretching surface. Magneto hydrodynamic (MHD) flow has important applications in MHD pumps, aerodynamics heating, MHD power generators, accelerators, purification of crude oil, petroleum industries and polymer technology [1]. Xinhua *et al.* [4] studied the asymmetric flow and heat transfer of viscous fluid between contracting/expanding rotating disks by using Homotopy analysis method. Siddique *et al.* [5] presented a new exact solution for MHD transient rotation flow of a second grade fluid in a porous space. Adabala Ramachandra Rao *et al.* [7] determined symmetric and asymmetric solutions of oscillatory MHD flow due to electrically rotating disks. Khan *et al.* [6] discussed MHD flows of a second grade fluid between two side walls perpendicular to a plate through a porous medium. Aziz *et al.* [9] discussed the thermal analysis of a longitudinal trapezoidal fin with temperature-dependent thermal conductivity and heat transfer coefficient. Abbasbandy [8] gave the application of Homotopy analysis method to nonlinear equation arising in heat transfer. Some exact solutions for the helical flow of a generalized Oldroyd-B fluid in a circular cylinder were presented by Fetecau *et al.* [10]. The purpose of this study is obtaining an analytical solution for radial velocity and axial velocity profiles on steady incompressible viscous MHD asymmetric flow of an electrically conducting fluid between two infinite parallel stationary coaxial porous disks of different permeability in the presence of a transverse magnetic field.

2. Mathematical formulation of the problem

Let us take the cylindrical polar coordinate system (r, θ, z) for the physical problem. Here, we consider the case of an asymmetric steady laminar incompressible viscous flow of an electrically conducting fluid confined between two large stationary porous disks of infinite radii coinciding with the planes $z = \pm a$ with constant injection velocities V_1 at the lower disk and V_2 at the upper disk in the presence of a uniform transverse magnetic field of intensities B_0 as shown in Fig. 1.

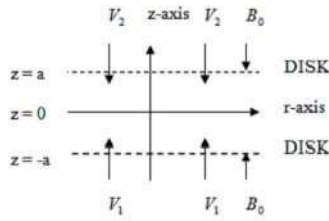


Fig 1: Geometry of the disks

To observe the effects of different permeability of the disks, we define the permeability parameter as follows:

$$A = 1 - \frac{V_1}{V_2} \tag{2.1}$$

With the presence of a uniform magnetic field, the governing equations for steady viscous flow of an electrically conducting fluid can be written as:

$$\frac{\partial \rho}{\partial t} + \nabla \cdot (\rho \underline{V}) = 0, \tag{2.2}$$

$$\frac{\partial \underline{V}}{\partial t} + (\underline{V} \cdot \nabla) \underline{V} = \underline{f} - \frac{1}{\rho} \nabla p + \nu \nabla^2 \underline{V}, \tag{2.3}$$

$$\nabla \cdot \underline{B} = 0, \tag{2.4}$$

$$\nabla \times \underline{B} = \mu_m \underline{J}, \tag{2.5}$$

$$\nabla \times \underline{E} = 0, \tag{2.6}$$

$$\underline{J} = \sigma_e (\underline{E} + \underline{V} \times \underline{B}), \tag{2.7}$$

Where ρ denotes the density, ∇ the gradient, \underline{V} the fluid velocity vector, ν kinematic viscosity, p the pressure, \underline{J} the current density, \underline{B} the total magnetic field so that $\underline{B} = \underline{B}_0 + \underline{b}$, \underline{b} the induced magnetic field, μ_m the magnetic permeability, \underline{E} the electric field, σ_e the electrical conductivity of the fluid and dot signifies the material derivative. Moreover $\nabla \cdot \underline{J} = 0$ is obtained from eqns. (2.4) and (2.5).

The uniform stationary magnetic field \underline{B} is in the transverse direction and the magnetic Reynolds number is taken small. As a consequence the induced magnetic field \underline{b} is neglected. We further assume that there is no electric field (i.e. $\underline{E} = 0$) as there is no applied polarization voltage. This means that no energy is extracted or added to the fluid system. By employing the above flow assumptions, the electromagnetic body force occurring in eqn. (2.3) takes the following linearized form:

$$\underline{f} = \underline{J} \times \underline{B} = \sigma_e [(\underline{V} \times \underline{B}_0) \times \underline{B}_0] = (-\sigma_e B_0^2 u, 0, 0). \tag{2.8}$$

The components of velocity (u, v, w) along radial, transverse and axial directions for the present problem can be written as:

$$u = u(r, z), v = 0, w = w(r, z). \tag{2.9}$$

In view of eqns. (2.4)-(2.8), the governing eqns. (2.2)-(2.3) for an electrically conducting incompressible fluid in the presence of a uniform magnetic field are given in dimensionless form as:

$$\frac{\partial u}{\partial r} + \frac{u}{r} + \frac{1}{a} \frac{\partial w}{\partial \eta} = 0, \tag{2.10}$$

$$\rho \left(u \frac{\partial u}{\partial r} + \frac{u}{a} \frac{\partial u}{\partial \eta} \right) = - \frac{\partial p}{\partial r} + \mu \left(\frac{\partial^2 u}{\partial r^2} + \frac{1}{r} \frac{\partial u}{\partial r} - \frac{u}{r^2} + \frac{1}{a^2} \frac{\partial^2 u}{\partial \eta^2} \right) - \sigma_e B_0^2 u, \tag{2.11}$$

$$\rho \left(u \frac{\partial w}{\partial r} + \frac{w}{a} \frac{\partial w}{\partial \eta} \right) = - \frac{1}{a} \frac{\partial p}{\partial \eta} + \mu \left(\frac{\partial^2 w}{\partial r^2} + \frac{1}{r} \frac{\partial w}{\partial r} + \frac{1}{a^2} \frac{\partial^2 w}{\partial \eta^2} \right), \tag{2.12}$$

Where $\eta = \frac{z}{a}$ is a similarity variable.

The boundary condition at the two porous disks for the velocity field is specified as follows:

$$\left. \begin{aligned} u(r, -1) = 0, \quad u(r, +1) = 0 \\ w(r, -1) = V_1, \quad w(r, +1) = V_2 \end{aligned} \right\} \tag{2.13}$$

Where V_1 and V_2 are uniform injection velocities at the lower and upper disks respectively.

A similarity transformation can be used to reduce partial differential equations (2.10)-(2.12) into ordinary differential equations as follows:

$$\psi(r, \eta) = \frac{V_2 r^2}{2} f(\eta), \tag{2.14}$$

$$u = \frac{1}{ra} \frac{\partial \psi}{\partial \eta} = \frac{V_2 r}{2a} f'(\eta), \tag{2.15}$$

$$w = -\frac{1}{r} \frac{\partial \psi}{\partial r} = -V_2 f(\eta), \tag{2.16}$$

The velocity components given in eqns. (2.15) and (2.16) are compatible with the continuity eqn. (2.10) and hence represent a possible fluid motion. Eqns. (2.11) and (2.12) in view of above similarity transformations (2.15) and (2.16) are reduced after eliminating the pressure term as follows:

$$f^{(iv)} + R(ff''' - M^2 f'') = 0, \tag{2.17}$$

Where $R = \frac{\rho}{\mu} V_2$ represents the Reynolds number and $M = \sqrt{\frac{\sigma_e a B_0^2}{\rho V_2}}$ is the Hartmann number.

Integrating eqn. (2.17) w.r.t η , we get

$$f''' + R(ff'' - \frac{f'^2}{2} - M^2 f') = k, \tag{2.18}$$

Where k is a constant of integration.

The boundary conditions (2.13) in dimensionless form can be written as:

$$\left. \begin{aligned} f(-1) = 1 - A, \quad f(1) = 1, \\ f'(-1) = 0, \quad f'(1) = 0. \end{aligned} \right\} \tag{2.19}$$

The shear stress on the disks is defined as:

$$T_w = -\mu \left(\frac{\partial u}{\partial z} \right)_{z=\pm a} = -\mu \frac{rV_2}{2a^2} f''(\pm 1). \tag{2.20}$$

We have to solve eqn. (2.18) subject to the boundary conditions (2.19).

3. Solution of the problem using the New Homotopy analysis method

New HAM is a non-perturbative analytical method for obtaining series solutions to nonlinear equations and has been successfully applied to numerous problems in science and engineering [14-29]. In comparison with other perturbative and non-perturbative analytical methods, New HAM offers the ability to adjust and control the convergence of a solution via the so-called convergence-control parameter. Because of this, New HAM has proved to be the most effective method for obtaining analytical solutions to highly non-linear differential equations. Previous applications of New HAM have mainly focused on non-linear differential equations in which the non-linearity is a polynomial in terms of the unknown function and its derivatives. As seen above, the non-linearity present in electro hydrodynamic flow takes the form of a rational function, and thus, poses a greater challenge with respect to finding approximate solutions analytically. Our results show that even in this case, New HAM yields excellent results. Liao [14-22] proposed a powerful analytical method for non-linear problems, namely the New Homotopy analysis method. This method provides an analytical solution in terms of an infinite power series. However, there is a practical need to evaluate this solution and to obtain numerical values from the infinite power series. In order to investigate the accuracy of the New Homotopy analysis method (New HAM) solution with a finite number of terms, the system of differential equations were solved. The New Homotopy analysis method is a good technique comparing to another perturbation method. The New Homotopy analysis method contains the auxiliary parameter h , which provides us with a simple way to adjust and control the convergence region of solution series. The approximate analytical solution of the eqns. (14)-(18) using the Homotopy analysis method [35] is

$$f(\eta) = -\frac{A\eta^3}{4} + \frac{3A\eta}{4} + \frac{2-A}{2} - hR \left[\frac{3A(\eta^4 - \frac{M^2\eta^5}{120} + \frac{M^2\eta^3}{60})}{2} - \frac{A}{8}\eta - \frac{AM^2}{80} - \frac{A}{16} \right] \tag{2.21}$$

The corresponding dimensionless radial velocity using the eqn. (2.21) is given by

$$f'(\eta) = -\frac{3A\eta^2}{4} + \frac{3A}{4} - hR \left[\frac{3A(\eta^3 - \frac{M^2\eta^4}{24} + \frac{M^2\eta^2}{20})}{2} - \frac{A\eta}{4} - \frac{AM^2}{80} \right] \tag{2.22}$$

And the shear stress using the eqn. (2.21) is given by

$$f''(\eta) = -\frac{3A\eta}{2} - hR \left[\frac{3A(\eta^2 - \frac{M^2\eta^3}{6} + \frac{M^2\eta}{10})}{2} - \frac{A}{4} \right] \tag{2.23}$$

4. Results and Discussion

In this section, we present our findings in tabular and graphical forms together with the discussion and their interpretations. The parameters of the study are Permeability parameter A , the Reynolds number R and the Hartmann number M . Fig. 1 illustrates the schematic diagram of geometry of the disks. Fig. 2, 4, 6 shows the dimensionless axial velocity $f(\eta)$ and Fig. 3, 5, 7 shows the dimensionless radial velocity $f'(\eta)$ w.r.to the similarity variable η respectively.

Fig. 2 depicts the velocity profile along axial direction. It is noted that increasing the permeability parameter A , lowers the axial velocity profile in some fixed values of the other parameter R and M . Fig. 3 shows that increasing the permeability parameter A , rises the radial velocity profile in some fixed values of the other parameter R and M . Fig. 4 shows that the axial velocity profile increases with increase in the magnitude of Reynolds number R and some fixed values of other parameter A and M . Fig. 5 depicts that increasing the magnitude of Reynolds number R , increases the radial velocity near the lower disk and decrease near the upper disk.

From Fig. 6, it is observed that the axial velocity profile increases near the lower disk and fall near the upper disk by increasing the values of the Hartmann number M and some fixed values of the other parameter A and R . From Fig. 7, it is noted that the radial velocity profile move towards the lower disk and it decreases by increasing the Hartmann number M and some fixed values of the other parameter A and R .

Table.1 shows the dimensionless axial velocity $f(\eta)$ for $A = 1.2, R = -20, M = 0.4$ using the eqn. (2.21) when $h = 0.098$. Table.2 depicts the shear stress at the disks for $R = -10, M = 0.8$ and various values of A using the eqn. (2.23) when $h = 0.096$. Table.3 infers the shear stress at the disks for $A = 1.4, M = 1.2$ and various values of R using the eqn.(2.23) when $h = 0.131$. Table.4 shows the shear stress at the disks for $A = 1.2, R = -20$ and various values of M using the eqn.(2.23) when $h = 0.142$.

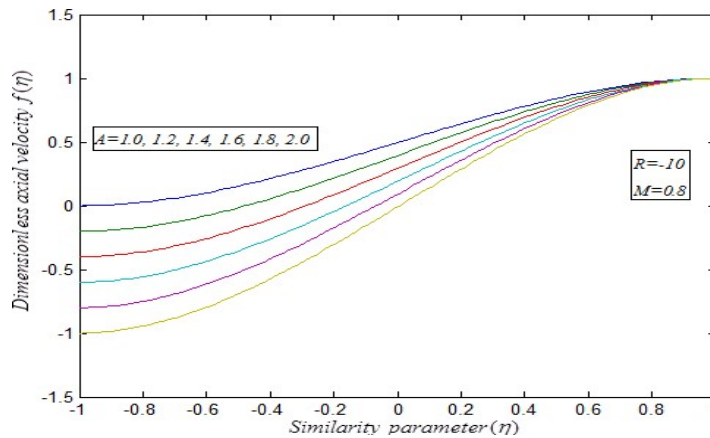


Fig 2: Dimensionless axial velocity $f(\eta)$ versus the Similarity parameter η . The curves are plotted for various values of the permeability parameter A and some fixed values of the other parameter R, M using the eqn. (2.21), when $h = -0.009$.

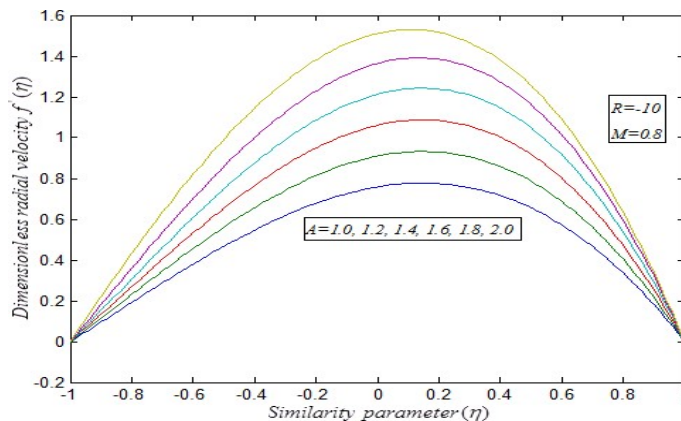


Fig 3: Dimensionless radial velocity $f'(\eta)$ versus the Similarity parameter η . The curves are plotted for various values of the permeability parameter A and some fixed values of the other parameter R, M using the eqn. (2.22), when $h = -0.09$.

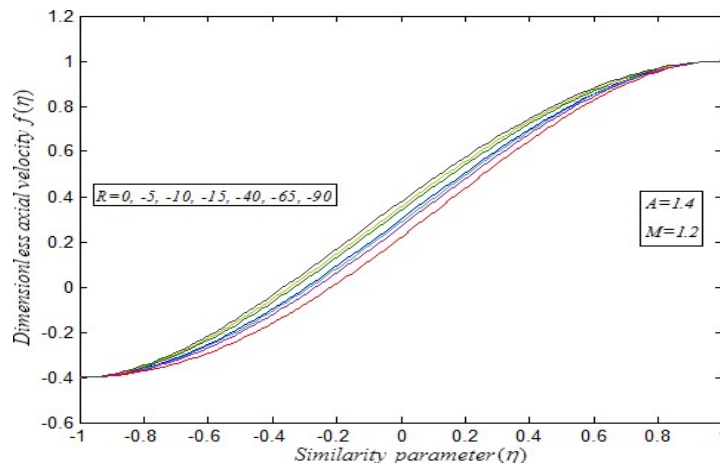


Fig 4: Dimensionless axial velocity $f(\eta)$ versus the Similarity parameter η . The curves are plotted for various values of the Reynolds number R and some fixed values of the other parameter A, M using the eqn. (2.21), when $h = 0.03$.

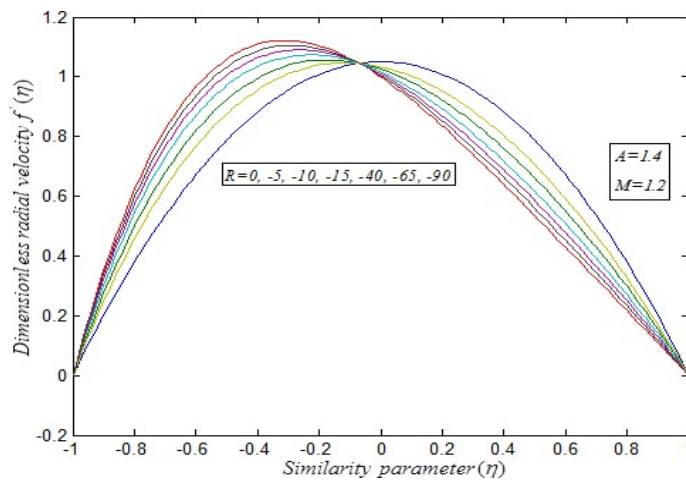


Fig 5: Dimensionless radial velocity $f'(\eta)$ versus the Similarity parameter η . The curves are plotted for various values of the Reynolds number R and some fixed values of the other parameter A, M using the eqn. (2.22), when $h = 0.09$.

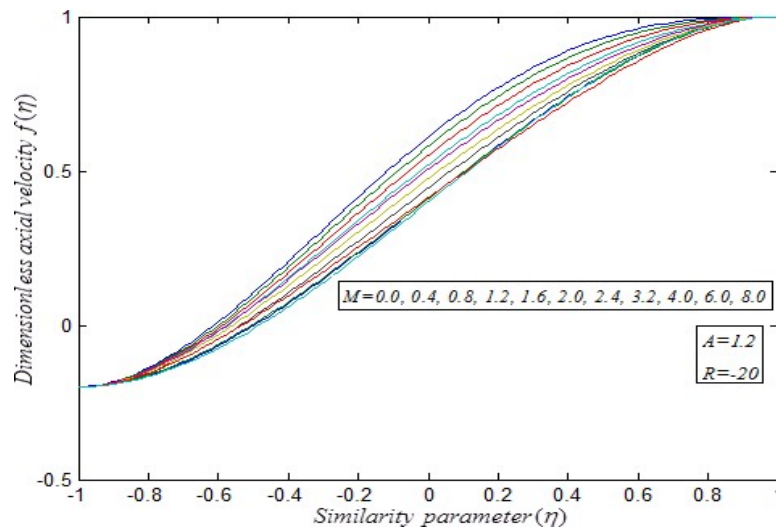


Fig 6: Dimensionless axial velocity $f(\eta)$ versus the Similarity parameter η . The curves are plotted for various values of the Hartmann number M and some fixed values of the other parameter A, R using the eqn. (2.21), when $h = 0.056$.

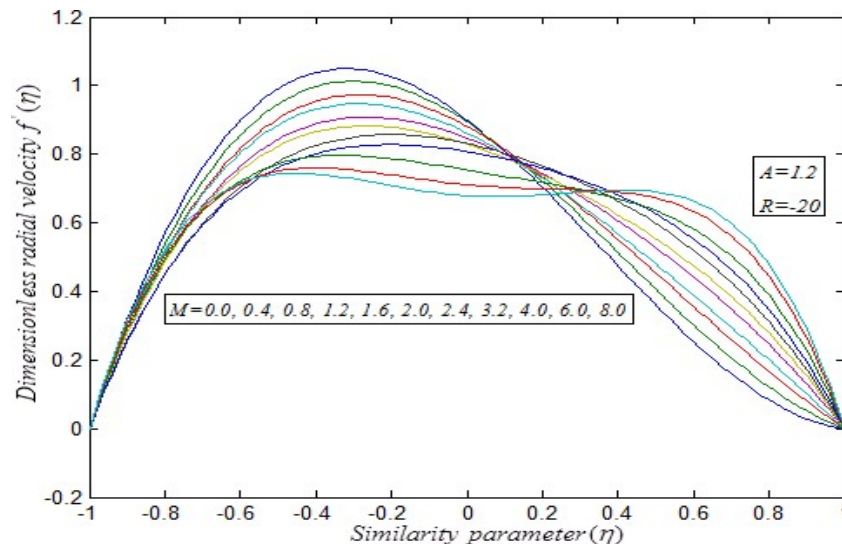


Fig 7: Dimensionless radial velocity $f'(\eta)$ versus the Similarity parameter η . The curves are plotted for various values of the Hartmann number M and some fixed values of the other parameter A, R using the eqn. (2.22), when $h = 0.065$.

Table 1: Dimensionless axial velocity $f(\eta)$ for $A = 1.2, R = -20, M = 0.4$ using the eqn. (2.21) when $h = 0.098$.

| | $f(\eta)$ |
|------|-----------|
| -1.0 | -0.200000 |
| -0.8 | -0.138745 |
| -0.6 | 0.156736 |
| -0.4 | 0.212504 |
| -0.2 | 0.408911 |
| 0 | 0.583750 |
| 0.2 | 0.730380 |
| 0.4 | 0.846612 |
| 0.6 | 0.931086 |
| 0.8 | 0.982596 |
| 1.0 | 1.00000 |

Table 2: Shear stresses at the disks for $R = -10, M = 0.8$ and various values of A using the eqn. (2.23) when $h = 0.096$.

| A | $f''(-1)$ | $-f''(1)$ |
|-----|-----------|-----------|
| 1.0 | 3.284214 | 0.928971 |
| 1.2 | 3.095395 | 1.182624 |
| 1.4 | 2.897496 | 1.471898 |
| 1.6 | 2.733888 | 1.804249 |
| 1.8 | 2.637869 | 2.178108 |
| 2.0 | 2.593920 | 2.593648 |

Table 3: Shear stresses at the disks for $A = 1.4, M = 1.2$ and various values of R using the eqn.(2.23) when $h = 0.131$.

| R | $f''(-1)$ | $-f''(1)$ |
|-----|-----------|-----------|
| 0 | 2.100000 | 2.100000 |
| -5 | 2.946467 | 1.906621 |
| -10 | 3.332487 | 1.889924 |
| -15 | 3.566543 | 1.883944 |
| -40 | 4.063685 | 1.872331 |
| -65 | 4.243910 | 1.868045 |
| -90 | 4.338195 | 1.865851 |

Table 4: Shear stresses at the disks for $A = 1.2$, $R = -20$ and various values of M using the eqn.(2.23) when $h = 0.142$.

| M | $f''(-1)$ | $-f''(1)$ |
|-----|-----------|-----------|
| 0.0 | 3.306960 | 0.799920 |
| 0.4 | 3.372768 | 0.880013 |
| 0.8 | 3.629797 | 1.124026 |
| 1.2 | 4.136174 | 1.529753 |
| 1.6 | 4.845108 | 2.075349 |
| 2.0 | 5.681304 | 2.732280 |
| 2.4 | 6.592160 | 3.473556 |
| 3.2 | 8.531228 | 5.131759 |
| 4.0 | 10.547424 | 6.939605 |
| 6.0 | 15.699492 | 11.779272 |
| 8.0 | 20.873808 | 16.803086 |

5. Conclusion

In this study, an analytical solution of the problem of MHD asymmetric flow of an electrically conducting fluid between two infinite parallel porous disks is investigated using a suitable similarity transformation. The analytical expressions of the dimensionless axial velocity and radial velocity have been derived by the Homotopy analysis method. In HAM, we can choose h in an appropriate way which controls the convergence of the series. This method can be easily extended to solve the non-linear initial and boundary value problems in physical sciences.

6. Acknowledgement

Researchers express their gratitude to the Secretary Shri S. Natanagopal, The Madura College Board, Madurai, Dr. K. M. Rajasekaran, The Principal and Dr. S. Muthukumar, Head of the Department of Mathematics, The Madura College (Autonomous), Madurai, Tamil Nadu, India for their constant support and encouragement.

7. References

- Muhammad A, Wehgal AR. MHD asymmetric flow between two porous disks, *Journal of Mathematics*, 44(2012): 9-21.
- Kashif A, Ahmad S, Muhammad A. On combined effect of thermal radiation and viscous dissipation in hydro magnetic micropolar fluid flow between two stretchable disks. Centre for Advanced studies in Pure and Applied Mathematics. Fang TS *et al.*, MHD and slip viscous flow over a stretching sheet. *Comm Nonlinear Sci Numerical Simulation*, 2009;14:3731-3737
- Xinhui S *et al.*, Homotopy analysis method for the asymmetric laminar flow and heat transfer of viscous fluid between contracting rotating disks. *Applied mathematical modeling*. 2012; 36:1806-1820.
- Siddique Mlieru D. A new exact solution for MHD transient rotation flow of a second grade Fluid in a Porous space. *Bulletin of the Polytechnic Institute*. 2008; 54: 27-36.
- Khan M, Hyder AS, Hayat T, Fetecau C. MHD flows of a second grade fluid between two side walls perpendicular to plate through a porous medium. *International Journal of Non-Linear Mechanics*. 2008; 43:302 – 319.
- Rao RA, Viswanathan SRK. Symmetric and asymmetric solutions of oscillatory MHD flow due to electrically rotating disks. *Journal of Indian Institute of Science*. 1987; 67:143-161.
- Abbasbandy S. The application of Homotopy analysis method to nonlinear equation arising in heat transfer. *Physics Letters A* 2006; 360:109-113.
- Khani F, Aziz A. Thermal analysis of a longitudinal trapezoidal fin with temperature-dependent thermal conductivity and heat transfer coefficient. *Communications in Nonlinear Science and Numerical Simulation*. 2010; 15:590-601.
- Fetecau C, Mahmood A, Fetecau C, Vieru D. Some exact solutions for the helical flow of a generalized Oldroyd-B fluid in circular cylinder. *Computers & Mathematics with Applications*. 2008; 56:3096-3108.
- Liao SJ. The proposed Homotopy analysis technique for the solution of non-linear Problems, *Ph.D. Thesis*, Shanghai JiaoTong University, 1992.
- Liao SJ. An approximate solution technique which does not depend upon small parameters: a special example. *Int J Non-Linear Mech*. 1995; 30:371-380.
- Liao SJ. Beyond perturbation introduction to the Homotopy analysis method, 1st edn. Chapman and Hall, CRC press, BocaRaton, 2003, 336.
- Liao SJ. On the Homotopy analysis method for nonlinear problems. *Appl Math Comput*. 2004; 147:499-513.
- Liao SJ. An optimal Homotopy-analysis approach for strongly nonlinear differential equations. *Commun Nonlinear Sci Numer Simulat*. 2010; 15:2003-2016.
- Liao SJ. The Homotopy analysis method in nonlinear differential equations. Springer and Higher education press, 2012.
- Liao SJ. An explicit totally analytic approximation of Blasius viscous flow problems. *Int J Nonlinear Mech*. 1999; 34:759–78.
- Liao SJ. On the analytic solution of magneto hydrodynamic flows non-Newtonian fluid over a stretching sheet. *J Fluid Mech*. 2003; 488:189–212.
- Liao SJ. A new branch of boundary layer flows over a permeable stretching plate. *Int J Nonlinear Mech*. 2007; 42:19–30.
- Domairry G, Bararnia H. An approximation of the analytical solution of some nonlinear heat transfer equations, a survey by using Homotopy analysis method. *Adv Studies Theor Phys*. 2008; 2:507-518.
- Tan Y, Xu H, Liao SJ. Explicit series solution of travelling waves with a front of Fisher equation. *Chaos Solitons Fractals*. 2007; 31:462–72.

21. Abbasbandy S. Soliton solutions for the Fitzhugh Nagumo equation with the Homotopy analysis method. *Appl Math Model.* 2008; 32:2706–14.
22. Cheng J, Liao SJ, Mohapatra RN, Vajravelu K. Series solutions of Nano boundary layer flows by means of the Homotopy analysis method. *J Math Anal Appl.* 2008; 343:233–245.
23. Hayat T, Abbas Z. Heat transfer analysis on MHD flow of a second grade fluid in a channel with porous medium. *Chaos Solitons Fractals.* 2008; 38:556–567.
24. Hayat T, Nazr R, Sajid M. On the Homotopy solution for Poiseuille flow of a fourth grade fluid. *Commun Nonlinear Sci Numer Simul.* 2010; 15:581–589.
25. Jafari H, Chun C, Saeidy SM. Analytical solution for nonlinear gas dynamic Homotopy Analysis method. *Appl Math.* 2009; 4:149–154.
26. Subha M, Ananthaswamy V, Rajendran L. Analytical solution of non-linear boundary value problem for the electrohydrodynamic flow equation. *International Journal of Automation and Control Engineering.* 2014; 3(2):48-56.
27. Saravanakumar K, Ananthaswamy V, Subha M, Rajendran L. Analytical Solution of nonlinear boundary value problem for in efficiency of convective straight Fins with temperature-dependent thermal conductivity, *ISRN Thermodynamics*, Article ID 28248, 2013, 1-18.
28. Ananthaswamy V, Subha M. Analytical expressions for exothermic explosions in a slab. *International Journal of Research–Granthaalayah.* 2014; 1(2):22-37.
29. Ananthaswamy V, Uma Maheswari S. Analytical expression for the hydrodynamic fluid flow through a porous medium. *International Journal of Automation and Control Engineering.* 2015; 4(2):67-76.
30. Ananthaswamy V, Sahaya Amalraj L. Thermal stability analysis of reactive hydromagnetic third-grade fluid using Homotopy analysis method. *International Journal of Modern Mathematical Sciences.* 2016; 14(1):25-41.
31. Ananthaswamy V, Iswarya T. Analytical expressions of mass transfer effects on unsteady flow past an accelerated vertical porous plate with suction. *Nonlinear studies.* 2016; 23(1):73-86.
32. Ananthaswamy V, Iswarya T. Analytical expressions of the effect of radiation on free convective flow of heat and mass transfer. *Nonlinear studies.* 2016; 23(1):133-147.
33. Ananthaswamy V, Kalaivani M. Mathematical expression of radiative radial fins with temperature-dependent thermal conductivity. *International Journal of Scientific Research and Modern Education.* 2016; 1(1).
34. Ananthaswamy V, Kalaivani M. A mathematical study of heat and mass transfer on non-linear MHD boundary layer flow. *American Journal of Engineering Science and Technology Research.* 2016; 4:1-17.

Appendix: A

Basic concept of the New Homotopy analysis method ^[11-35]

Consider the following differential equation:

$$N[u(t)] = 0 \tag{A.1}$$

Where N is a nonlinear operator, t denote an independent variable, $u(t)$ is an unknown function. For simplicity, we ignore all boundary or initial conditions, which can be treated in the similar way. By means of generalizing the conventional Homotopy method, Liao (2012) constructed the so-called zero-order deformation equation as:

$$(1 - p)L[\varphi(t; p) - u_0(t)] = phH(t)N[\varphi(t; p)] \tag{A.2}$$

where $p \in [0,1]$ is the embedding parameter, $h \neq 0$ is a nonzero auxiliary parameter, $H(t) \neq 0$ is an auxiliary function, L an auxiliary linear operator, $u_0(t)$ is an initial guess of $u(t)$, $\varphi(t; p)$ is an unknown function. It is important to note that one has great freedom to choose auxiliary unknowns in HAM. Obviously, when $p = 0$ and $p = 1$, it holds:

$$\varphi(t;0) = u_0(t) \text{ and } \varphi(t;1) = u(t) \text{ respectively.} \tag{A.3}$$

Thus, as p increases from 0 to 1, the solution $\varphi(t; p)$ varies from the initial guess $u_0(t)$ to the solution $u(t)$. Expanding $\varphi(t; p)$ in Taylor series with respect to p , we have:

$$\varphi(t; p) = u_0(t) + \sum_{m=1}^{+\infty} u_m(t)p^m \tag{A.4}$$

Where

$$u_m(t) = \frac{1}{m!} \left. \frac{\partial^m \varphi(t; p)}{\partial p^m} \right|_{p=0} \tag{A.5}$$

If the auxiliary linear operator, the initial guess, the auxiliary parameter h , and the auxiliary function are so properly chosen, the series (A.4) converges at $p=1$ then we have:

$$u(t) = u_0(t) + \sum_{m=1}^{+\infty} u_m(t). \tag{A.6}$$

Differentiating (A.2) for m times with respect to the embedding parameter p , and then setting $p = 0$ and finally dividing them by $m!$, we will have the so-called m th-order deformation equation as:

$$L[u_m - \chi_m u_{m-1}] = hH(t)\mathfrak{R}_m(u_{m-1}) \tag{A.7}$$

Where

$$\mathfrak{R}_m(u_{m-1}) = \frac{1}{(m-1)!} \frac{\partial^{m-1} N[\varphi(t; p)]}{\partial p^{m-1}} \quad (\text{A.8})$$

And

$$\chi_m = \begin{cases} 0, & m \leq 1, \\ 1, & m > 1. \end{cases} \quad (\text{A.9})$$

Applying L^{-1} on both side of equation (A7), we get

$$u_m(t) = \chi_m u_{m-1}(t) + hL^{-1} [H(t)\mathfrak{R}_m(u_{m-1})] \quad (\text{A.10})$$

In this way, it is easily to obtain u_m for $m \geq 1$, at M^{th} order, we have

$$u(t) = \sum_{m=0}^M u_m(t) \quad (\text{A.11})$$

When $M \rightarrow +\infty$, we get an accurate approximation of the original equation (A.1). For the convergence of the above method we refer the reader to Liao [20]. If equation (A.1) admits unique solution, then this method will produce the unique solution.

Appendix B

Approximate analytical expressions of the non-linear differential eqns. (2.17)-(2.20) using the New Homotopy analysis method

$$f^{(iv)} + R(ff''' - M^2 f'') = 0, \quad (\text{B.1})$$

We construct the Homotopy for the eqn. (B.1) as follows:

$$(1-p) f^{(iv)} - hp f^{(iv)} + R(ff''' - M^2 f'') = 0 \quad (\text{B.2})$$

The approximate solution of the eqns. (B.2) as follows:

$$f = f_0 + pf_1 + p^2 f_2 + p^3 f_3 + \dots \quad (\text{B.3})$$

Substituting the eqns. (B.3) in the eqn. (B.2), we get

$$(1-p) \left[\frac{d^4(f_0 + pf_1 + p^2 f_2 + p^3 f_3 + \dots)}{d\eta^4} \right] - hp \left[\frac{d^4(f_0 + pf_1 + p^2 f_2 + p^3 f_3 + \dots)}{d\eta^4} \right] + R \left[\frac{d^3(f_0 + pf_1 + p^2 f_2 + p^3 f_3 + \dots)}{d\eta^3} \left(\frac{d^2(f_0 + pf_1 + p^2 f_2 + p^3 f_3 + \dots)}{d\eta^2} \right) - M^2 \frac{d^2(f_0 + pf_1 + p^2 f_2 + p^3 f_3 + \dots)}{d\eta^2} \right] = 0 \quad (\text{B.4})$$

Comparing the coefficients of like powers of p in the eqns. (B.4), we get

$$p^0 : \frac{d^4 f_0}{d\eta^4} = 0 \quad \left[\frac{d^3 f_0}{d\eta^3} \quad \frac{d^2 f_0}{d\eta^2} \right] \quad (\text{B.5})$$

$$p^1 : \frac{d^4 f_1}{d\eta^4} = h \left[R \left(\frac{d^3 f_0}{d\eta^3} \frac{d^2 f_0}{d\eta^2} - M^2 \frac{d^2 f_0}{d\eta^2} \right) \right] \quad (\text{B.6})$$

The initial approximations are as follows:

$$f_0(-1) = 1 - Af'(-1) \quad f_0(1) = 1, \quad f_0'(-1) = 0, \quad f_0'(1) = 0, \quad (\text{B.7})$$

$$f_i(-1) = 0, \quad f_i(1) = 0, \quad f_i'(-1) = 0, \quad f_i'(1) = 0, \quad \text{where } i = 1, 2, 3, \dots \quad (\text{B.8})$$

Solving the eqns. (B.5), (B.6) and using the boundary conditions (B.7) and (B.8) we can obtain the following results:

$$f_0(\eta) = -\frac{A\eta^3}{4} + \frac{3A\eta}{4} + \frac{2-A}{2} \quad (\text{B.9})$$

$$f_1(\eta) = R \left[\frac{3A}{24} \left(\eta^4 - \frac{M^2 \eta^5}{120} - \frac{M^2 \eta^3}{60} \right) - \frac{A}{8} \eta - \frac{AM^2}{80} \eta + \frac{A}{16} \right] \quad (\text{B.10})$$

According to the Homotopy analysis method we have

$$f = \lim_{p \rightarrow 1} f(\eta) = f_0 + f_1 \quad (\text{B.11})$$

Using the eqns. (B.9) and (B.10) in (B.11), we obtain the solutions in the text as given in the eqns. (2.17)–(2.20).

Appendix: C
Nomenclature

| Symbols | Meaning |
|-----------------|--|
| A | Permeability parameter |
| B_0 | Magnetic field intensity |
| \underline{b} | Induced magnetic field |
| \underline{E} | Electric field |
| \underline{J} | Current density |
| k | Constant of integration |
| M | Hartmann number |
| R | Reynolds number |
| TOL_{iter} | Prescribed error tolerance |
| V_1, V_2 | Injection velocities at the lower and upper disks respectively. |
| u, w | Velocity components along the radial and axial directions respectively |
| | Similarity parameter |
| | Density |
| | Viscosity |
| ν | Kinematic viscosity |
| Ψ | Stream function |
| σ_e | Electrical conductivity |
| μ_m | Magnetic permeability |